

Non-oxide sol-gel synthesis of terbium doped silicon nitride phosphors^a

Shereen Hassan, Marina Carravetta, Andrew L. Hector^{*} and Laura A. Stebbings

School of Chemistry, University of Southampton, Highfield, Southampton SO17 1BJ, UK

Abstract

Exposure of solutions of $\text{Tb}(\text{N}(\text{SiMe}_3)_2)_3$ with $\text{SiCl}(\text{NEt}_2)_3$ in THF to dry ammonia results in polymeric xerogels. Heating these gels in ammonia leads to amorphous $\text{Tb}:\text{SiN}_x$ phosphors that exhibit bright green luminescence under UV irradiation. MAS-NMR and combustion analysis show the phosphors to be silicon nitride materials analogous to those typically produced by sol-gel routes. Photoluminescence behavior is similar to that of $\text{Tb}:\text{SiN}_x$ or $\text{Tb}:\text{SiO}_2$ films produced by ion implantation that show good electroluminescence activity.

Introduction

Much of the interest in rare earth doped silicon nitride and oxynitride materials is related to potential applications as highly stable, efficient phosphors. The stability of these materials is based on their strongly bonded structures based on networks of covalent SiN_4 units. Attention has focused on use as down-conversion phosphors for solid state lighting based on blue, NUV or UV LEDs,¹⁻³ providing white light sources with high efficiency (%) and efficacy (lm/W) so promising large energy savings by replacement of incandescent and fluorescent lamps. Recently there has also been interest in producing rare earth doped silicon nitride films as emitters. Rare earth doped SiO_2 is an effective source of light emission,⁴ but the large bandgap of SiO_2 leads to

^a Supported by the Egyptian government (study fellowship to SH) and the Royal Society (University Research Fellowships to MC and ALH)

^{*} A.L.Hector@soton.ac.uk

inefficient carrier injection and electroluminescence based on these materials depends on excitation by impact of high energy electrons.⁵ High working temperatures, device degradation and incompatibility with some technologies are the result. Tb^{3+} implantation into PECVD-grown silicon nitride was shown to result in significantly higher quantum efficiency of photoluminescence from the terbium ions.⁵ Similarly Er^{3+} -doped silicon nitride films produced by a co-sputtering method show strong photoluminescence.⁶ There have also been studies of rare earth doping into other nitrides. BN based phosphors have been proposed for use in extreme environments such as high temperatures and high radiation levels.⁷ Tm, Tb, Sm, Eu or Yb doped AlN films have been produced using reactive radiofrequency sputtering and show strong photoluminescence and cathodoluminescence.⁸ Eu^{2+} doped AlN shows stronger blue cathodoluminescence than the $\text{Ce}^{3+}:\text{Y}_2\text{SiO}_5$ blue phosphor normally used in field emission displays.⁹ There are various other reports of high emission efficiencies from rare earth centers in III-nitride matrices, largely for field emission applications.¹⁰⁻¹³

Advantages of sol-gel methods in materials synthesis include lower cost than vapor deposition techniques, they can also readily be used to coat very large areas, or to produce morphologies such as films with ordered pore structures, or monolithic materials. Oxide or fluoride based phosphors can readily be produced by doping lanthanide ions into sols.¹⁴ Sol-gel routes to nitride materials¹⁵ are poorly developed due to the air sensitivity of the chemistry involved at each step of the process. This sensitivity is due to the need to base the processing on nitrogen donor groups such as amides, which are readily displaced by water. Published work is largely focused on the production of high surface area silicon nitride powders for catalysis¹⁶ and Si/B/C/N ceramics.¹⁷ Recently there have been reports of the production of silicon nitride or

carbonitride membranes¹⁸ and we have reported the formation of films,¹⁹ monolithic gels,²⁰ aerogels²⁰ and inverse opals²¹ in nitride materials.

For silicon nitride-based phosphors a sol-gel route offers better control and homogeneity in the rare earth concentration than when ion implantation methods are used since the concentration in the sol is directly related to that in the powder or film. The accurate doping of more than one rare earth or of rare earth/transition metal combinations (e.g. to produce phosphorescent materials or to mix emission colors) and an expansion of the range of forms in which these materials can be produced beyond powders and films, are possible outcomes. It also offers an opportunity to produce morphologies other than films, including periodic structures of potential interest as photonic materials.²¹ The use of such routes to incorporate other ions into silicon nitride and hence modify its properties is also a general interest. Jansen²² that showed B, Ti or Ta could be doped into SiN_x by adding the respective dimethylamide to the reaction between $\text{Si}(\text{NHMe})_4$ and ammonia. These silicon nitride materials are referred to as SiN_x rather than Si_3N_4 because they are amorphous materials with composition that deviates from Si_3N_4 , similar to the vapor deposited SiN_x films extensively used as capping layers and dielectrics in electronics. Amorphous ceramic metal/boron silicon nitrides were formed after annealing in NH_3 at 1000 °C while calcining at 1500 °C in N_2 atmosphere partially crystallized nanoparticles of the metal nitrides (TiN/TaN) which were distributed in the amorphous silicon metal nitride matrix. Others have incorporated Al^{23} or Ti^{24} into silicon nitride using single source precursors designed so that the active groups are amide ligands attached to silicon.

It has been shown that rare earth *tris(bis-trimethylsilyl)amides* react with ammonia to produce polymers which decompose on heating to yield the rare earth nitrides.²⁵ In this paper we investigate the doping of Tb³⁺ ions into silicon nitride starting from mixtures of Tb(N(SiMe₃)₂)₃ and SiCl(NEt₂)₃ in solution, and examine the composition, morphology and photoluminescence behavior of the products.

Experimental

All procedures were carried out under nitrogen using standard Schlenk techniques or a nitrogen filled glove box. Tetrahydrofuran (THF) was distilled from sodium:benzophenone and diethylamine from barium oxide. SiCl₄ and Li(N(SiMe₃)₂) were obtained from Aldrich and TbCl₃ from Strem. Anhydrous ammonia was obtained from Air Products and further dried by passing through a column of molecular sieves. SiCl(NEt₂)₃ was prepared by adding HNEt₂ (100 cm³) to a solution of SiCl₄ (10 cm³) in THF (40 cm³) at 0 °C. The mixture was stirred for 12 h, the HNMe₂.HCl precipitate was removed by filtration and the solvent removed *in vacuo* to obtain the crude product. This was purified by vacuum distillation (0.05 mm Hg) at ~75 °C. Yield 8.7 g, 52%. ¹H NMR (C₆D₆, 298 K): δ = 2.89 (q) CH₂ [2H], 0.95 (t) CH₃ [3H]. ¹³C{¹H} NMR (C₆D₆, 298 K): δ = 39.8 CH₂, 14.8 CH₃. Tb(N(SiMe₃)₂)₃ was obtained by the method described by Bradley.²⁹

To prepare the xerogels a solution of Tb(N(SiMe₃)₂)₃ (0.03, 0.035, 0.04, 0.045, 0.05, 0.055, 0.06 or 0.065 g in 10 cm³ THF) was mixed with solution of SiCl(NEt₂)₃ (0.5 cm³ / 0.53 g in 10 cm³ THF). Dry ammonia was flowed over the stirred mixture for 1 hr. The resultant precipitate was collected by filtration and dried *in vacuo*, then pyrolysed at 800 °C under flowing dry ammonia.

Calculated compositions based on the synthesis range from 1.7 to 3.7 at% Tb, but the measured compositions (EDX) are referred to in the text, these range from 2.1-4.6 at%.

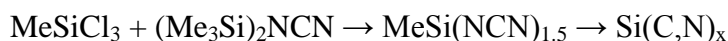
Solution NMR spectra were collected with a Bruker AV300 spectrometer. Solid state MAS-NMR were recorded with a Varian Infinity+ spectrometer at 9.4 T. The sample was placed in a 4 mm zirconia rotor and spun about the magic-angle at a 6.5 KHz spinning frequency using nitrogen gas to keep the sample in an inert atmosphere for the duration of the experiments. Spectra were referenced against silicon rubber (-22.3 ppm³⁰) and collected through direct observation (178 scans, 900 s relaxation) or after 5 ms ramped cross-polarization (128 scans, 5 s relaxation),³¹ without proton decoupling. Powder X-ray diffraction measurements were carried out using a Siemens D5000 diffractometer with Cu-K_{α1} radiation. Thermogravimetric analysis used a Mettler Toledo TGA851e housed in a glove box and supplied with Air Products BiP grade nitrogen. IR spectra were collected as CsI disks held in a nitrogen filled cell on a Perkin Elmer Spectrum 1 spectrometer. SEM images were obtained with a Jeol JSM-5910 microscope using carbon coated samples, EDX spectra were collected with an Oxford Instruments Inca probe. TEM samples were prepared by dispersing the material into toluene with ultrasound then placing a drop onto a carbon coated grid and allowing to evaporate, images were collected at 300 kV with a Jeol JEM-3010 microscope. Photoluminescence spectra were collected on neat or NaCl-diluted phosphor samples with a Perkin Elmer LS55 spectrometer. Combustion analysis data were obtained commercially through Medac Ltd with a Thermo1112 Flash elemental analyzer. It is difficult to recover all the nitrogen from Si₃N₄, but after trying various conditions the samples were analyzed using the most effective method found: samples were loaded into tin capsules with WO₃ added as a combustion aid.

Results and Discussion

A number of different precursors could potentially be used in sol-gel processes to yield silicon nitride. The obvious approach is to react a silicon amide with ammonia yielding a polymeric network containing Si-NH-Si bridging groups:



This approach has been used by Bradley¹⁶ using $Si(NH_2)(NMe_2)_3$ and by Jansen²² with $Si(NHMe)_4$. A further variation is to use other nitrogen containing bridging groups such as $(NCN)^{2-}$, as used by Kroke and co-workers¹⁶ to make carbonitrides:



In order to ensure Tb:SiN_x ceramics with an even distribution of Tb ions through the lattice it was decided in this work to use a silicon precursor that readily precipitated on exposure to ammonia. Initially Tb(N(SiMe₃)₂)₃ was mixed with Si(NHMe)₄ or Si(NMe₂)₄ in THF solution and exposed to dried ammonia. The products were oils or oily solids even after an extended exposure to dry ammonia and it was concluded that these precursors were too unreactive to be useful. Si(NHMe)₄ leads to solid xerogels when a trifluoromethanesulfonic acid catalyst is used²⁰ and may be suitable for production of phosphors similar to those described herein, but was not used here due to concern that Tb ions would not be immobilized in the oily products and so Tb rich regions could form. Previous studies by others²² used a 1:1 or 1:2 ratio of boron or transition metal amide:Si(NHMe)₄ and these did lead to solid xerogels. It is likely that the second element (B or metal) underwent condensation reactions more readily resulting in a larger

oligomer size and therefore a solid product and that this does not occur with the very low doping levels used herein.

$\text{SiCl}(\text{NEt}_2)_3$ is simple to prepare and purify, and precipitation occurs rapidly on exposing it to ammonia in THF solution. Gels were prepared with varying concentrations of Tb^{3+} ions, fired to ceramic materials under ammonia at 800 °C and the variation in the photoluminescence with Tb^{3+} concentration measured.

TGA of the xerogels under N_2 showed a sharp 60% mass loss around 200 °C corresponding to loss of the amine hydrochloride by-product and some further condensation of the xerogel, followed by a slow mass loss of a further 14% which was complete by 800 °C. IR spectra, Fig. 1, contained a broad band centered at 3136 cm^{-1} ($\nu_{\text{N-H}}$) and peaks at $2850\text{--}2720\text{ cm}^{-1}$ ($\nu_{\text{C-H}}$), 1448 (δ_{NH_2}), 1405 cm^{-1} ($\nu_{\text{C-N}}$), 1200 and 916 cm^{-1} ($\nu_{\text{Si-N}}$). Other peaks corresponding to $\text{HNEt}_2\cdot\text{HCl}$ were also seen. This is consistent with the expected reaction scheme for ammonolysis of the silicon reagent:



IR spectra of the ceramic products after pyrolysis at 800 °C (Fig. 1) showed $\nu_{\text{N-H}}$ at 3348 cm^{-1} , $\nu_{\text{C}\equiv\text{N}}$ at 2157 cm^{-1} , δ_{NH_2} at 1453 cm^{-1} and a broad, intense $\nu_{\text{Si-N}}$ peak at 978 cm^{-1} . No evidence of residual organic groups ($\nu_{\text{C-H}}$) was found. This closely resembles spectra of silicon nitride samples produced by heating $\text{Si}(\text{NH}_2)(\text{NMe}_2)_3/\text{NH}_3$ -derived gels under similar conditions, where the presence of the $\nu_{\text{C}\equiv\text{N}}$ peak was attributed to pyrolysed organic substituent groups.²⁶ Powder

X-ray diffraction showed the fired ceramic materials to be amorphous and TGA showed that when heated under N₂ it underwent no further mass loss.

Solid state ²⁹Si MAS-NMR showed a single strong peak with a maximum between -43.7 and -45.5 ppm, Fig. 2. This is particularly significant as MAS-NMR is particularly sensitive to oxide incorporation into silicon nitride – every oxygen atom results in three SiN₃O tetrahedra. Recently we produced silicon nitride xerogels from another route and detected low level oxide contamination in these through the observation of SiN₄, SiN₃O, SiN₂O₂ and SiNO₃ groups.²⁰ The chemical shift observed for the xerogels produced herein is consistent with SiN₄ and no other environments are seen. A significant signal enhancement was observed using cross polarization, though the appearance of the spectrum did not change. This shows that many silicon centers are still close to protons as expected in these gel-derived materials. Combustion microanalysis resulted in a nitrogen content of 35.1-35.7%, 2% hydrogen and no detectable carbon. Si₃N₄ contains 40% N so these SiN_x films are slightly N deficient. No Cl was observed by EDX in any of the fired samples.

SEM of the fired samples showed large spherical particles with diameters of ~0.5-1.5 μm with powdery material, Fig. 3. This spherical morphology is similar to that often obtained when SiO₂ is grown under basic conditions (the Stöber process).²⁷ EDX showed the spherical and powdery material to have similar Tb concentrations within each sample. The measured Tb:Si ratios were around 25% higher than expected from the reagent mix and thus the measured compositions have been used to describe samples herein. Presumably the loss of some low molecular weight silicon oligomers during the firing process leads to samples richer in Tb than expected. The EDX probe

in the SEM used does not detect N due to absorption from the BN window but a strong nitrogen signal was observed in the EDX when measured in the TEM. Imaging in the TEM, Fig. 4, showed the sample to be of homogenous density and amorphous. No nanoparticles were observed as might be expected if phase segregation was occurring and the more sinterable TbN component started to crystallize.

Fired samples were found to emit high intensity green light under UV irradiation with a 240 nm lamp. Photoluminescence spectra on the solids (Fig. 5) showed the characteristic lines associated with the Tb^{3+} ion. A small degree of Stark splitting is observed on the $^5\text{D}_4 \rightarrow ^7\text{F}_5$ line but the overall linewidths are relatively narrow, suggesting that Tb^{3+} ions are all in similar high symmetry environments. The comparison in Table 1 shows similar positions for these lines to those found in other nitride materials doped with Tb^{3+} and also to Tb^{3+} doped SiO_2 . No significant shift in the positions due to the nitride lattice is observed and the peak positions are even comparable with those observed for the $\text{Tb}^{3+}_{(\text{aq})}$ ion.²⁸ This is not uncommon with rare earth ions since the *f*-electrons are relatively well shielded from the host lattice. The MAS-NMR and IR suggest that the samples studied herein contain little oxygen but there was some concern that small amounts of oxygen might be incorporated into the lattice and be preferentially coordinated to the oxophilic Tb^{3+} ions. For the samples described above the anhydrous grade ammonia was passed through a 70 cm column of dried molecular sieves to remove trace water, but to check the effect of moisture a sample was fired under undried ammonia. The PL spectrum of this 3.55 at% Tb sample showed a 26% weaker $^5\text{D}_4 \rightarrow ^7\text{F}_6$ line than the sample heated under dried NH_3 . This suggests that a higher oxygen content reduces the efficiency of the phosphors and that Tb is mainly N-coordinated in these materials. This conclusion is supported by the

previous observation that Tb^{3+} photoluminescence in SiO_2 films is much weaker than similar concentrations in SiN_x films.⁵

The excitation spectrum has maxima at 224, 242 and 257 nm but with strong excitation at all wavelengths up to ~270 nm. The sample couples well with a standard 240 nm UV lamp (Fig. 5). One feature of nitride phosphors that is useful for solid state lighting is that the excitation range can often extend into the near UV or the blue region of the visible spectrum, allowing coupling to GaN based LEDs. These phosphors would not be useful for these applications. However, the range of wavelengths in which excitation occurs is comparable to Tb^{3+} implanted SiN_x films^{5,6} that have been investigated as the basis of Si-based emitters with tunneling electrons causing electroluminescence.

Fig. 6 shows the variation of the emission intensity from these phosphors with the Tb concentration. The $^5\text{D}_4 \rightarrow ^7\text{F}_6$ line was used so that undiluted samples could be studied (the $^5\text{D}_4 \rightarrow ^7\text{F}_5$ was off-scale with all slit combinations). The intensity of emission is seen to increase with Tb content until it reaches a maximum at around 3.5 at% (the most intense sample was produced using 0.05 g $\text{Tb}(\text{Si}(\text{NMe}_2)_3)_3$ with 0.5 cm^3 $\text{SiCl}(\text{NEt}_2)_3$). At higher concentrations quenching was observed to cause a reduction in the photoluminescence intensity.

Conclusions

Terbium doping of silicon nitride is possible by a sol-gel type route, with $\text{SiCl}(\text{NEt}_2)_3$ an effective starting material for producing phosphors in powdered form since rapid precipitation with ammonia can immobilize Tb ions in the nitride lattice. Firing the precipitate under

ammonia results in phosphors with bright green emission under UV illumination. The frequencies of the Tb^{3+} emission lines are similar to those seen in oxides, so there is no shift due to the different electronegativity of the lattice ions, but similarly to ion implanted SiN_x lattices, the emission intensity is higher compared to SiO_2 systems. Sol-gel approaches are versatile in the range of product morphologies that they can be used to access. Hence homogeneous SiN_x films could be produced relatively cheaply with good control over the content of the luminescent ion. There is also an interest in producing optical materials in other forms and this versatile technique could be used to access some of these, such as aerogels and other porous structures.

Acknowledgements

Thanks to Barbara Cressey for collecting the TEM data, to Malcolm Levitt for providing access to the NMR and N_2 evaporation facilities and to Richard Morris (MEDAC Ltd) for optimizing the combustion regimes used in sample analysis.

References

- 1 R.-J. Xie and N. Hirosaki, "Silicon-based oxynitride and nitride phosphors for white LEDs - a review," *Sci. Tech. Adv. Mater.*, **8** [7-8], 588-600 (2007).
- 2 C. Feldmann, T. Jüstel, C. R. Ronda and P. J. Schmidt, "Inorganic luminescent materials: 100 years of research and application," *Adv. Inorg. Mater.*, **13** [7], 511-516 (2003).
- 3 R. Mueller-Mach, G. Mueller, M. R. Krames, H. A. Höppe, F. Stadler, W. Schnick, T. Juestel and P. Schmidt, "Highly efficient all-nitride phosphor-converted white light emitting diode," *Phys. Stat. Sol. A-Appl. Mater. Sci.*, **202** [9], 1727-1732 (2005).

- 4 H. Amekura, A. Eckau, R. Carius and Ch. Buchal, "Room-temperature photoluminescence from Tb ions implanted in SiO₂ on Si," *J. Appl. Phys.*, **84** [7], 3867-3871 (1998).
- 5 Z. Yuan, D. Li, M. Wang, P. Chen, D. Gong, L. Wang and D. Yang, "Photoluminescence of Tb³⁺ doped SiN_x films grown by plasma-enhanced chemical vapor deposition," *J. Appl. Phys.*, **100** [8], 083106 4pp (2006); Z. Yuan, D. Li, M. Wang, D. Gong, P. Cheng, P. Chen and D. Yang, "Photoluminescence of Tb³⁺-doped SiN_x films with different Si concentrations," *Mater. Sci. Eng. B*, **146** [1-3] 126-130 (2008).
- 6 M. J. V. Bell, L. A. O. Nunes and A.R. Zanatta, "Optical excitation of Er³⁺ ions in *a*-SiN alloys," *J. Appl. Phys.*, **86** [1], 338-341 (1999).
- 7 E. M. Shishonok, S. V. Leonchik and J. W. Steeds, "Luminescence from europium, europium-chromium, erbium, samarium and terbium-activated powder, ceramic and polycrystalline cubic boron nitride," *Phys. Stat. Sol. B-Basic Sol. St. Phys.*, **244** [6], 2172-2179 (2007).
- 8 R. Weingärtner, O. Erlenbach, A. Winnacker, A. Welte, I. Brauer, H. Mendel, H. P. Strunk, C. T. M. Ribeiro and A. R. Zanatta, "Thermal activation, cathodo- and photoluminescence measurements of rare earth doped (Tm, Tb, Dy, Eu, Sm, Yb) amorphous/nanocrystalline AlN thin films prepared by reactive rf-sputtering," *Opt. Mater.*, **28** [6-7], 790-793 (2006).
- 9 N. Hirosaki, R.-J. Xie, K. Inoue, T. Sekiguchi, B. Dierre and K. Tamura, "Blue-emitting AlN:Eu²⁺ nitride phosphor for field emission displays," *Appl. Phys. Lett.*, **91** [6], 061101 3pp (2007).
- 10 B. Han, K. C. Mishra, M. Raukas, K. Klinedinst, J. Tao and J. B. Talbot, "A study of luminescence from Tm³⁺, Tb³⁺, and Eu³⁺ in AlN powder," *J. Electrochem. Soc.*, **154** [9], J262-J266 (2007).

- 11 F. S. Liu, W. J. Wa, Q. L. Liu, J. K. Liang, J. Luo, L. T. Yang, G. B. Song, Y. Zhang and G. H. Rao, "Photoluminescence and characteristics of terbium-doped AlN film prepared by magnetron sputtering," *Appl. Surf. Sci.*, **245** [1-4], 391-399 (2005).
- 12 H. Mendel, S. B. Aldabergenova, R. Weingärtner, G. Frank, H. P. Strunk and A. A. Andreev, "Annealing of amorphous and nanocrystalline AlN and GaN films and photoluminescence of Tb³⁺ centers," *Opt. Mater.*, **28** [6-7], 794-796 (2006).
- 13 A. Podhorodecki, M. Nyk, J. Misiewicz and W. Strek, "Optical investigation of the emission lines for Eu³⁺ and Tb³⁺ ions in the GaN powder host," *J. Lumin.*, **126** [1], 219-224 (2007).
- 14 A. A. Ismail, M. Abboudi, P. Holloway and H. El-Shall, "Photoluminescence from terbium doped silica-titania prepared by a sol-gel method," *Mater. Res. Bull.*, **42** [1], 137-142 (2007); S. Lepoutre, D. Boyer and R. Mahiou, "Structural and optical characterizations of sol-gel based fluorides materials: LiGdF₄:Eu³⁺ and LiYF₄:Er³⁺," *Opt. Mater.*, **28** [6-7], 592-596 (2006).
- 15 A. L. Hector, "Materials synthesis using oxide free sol-gel systems," *Chem. Soc. Rev.*, **36** [11], 1745-1753 (2007).
- 16 R. Rovai, C. W. Lehmann and J. S. Bradley, "Non-oxide sol-gel chemistry: Preparation from tris(dialkylamino)silazanes of a carbon-free, porous, silicon diimide gel," *Angew. Chem. Intl. Ed.*, **38** [13-14], 2036-2038 (1999); F. Cheng, S. J. Archibald, S. Clark, B. Toury, S. M. Kelly and J. S. Bradley, "Preparation of mesoporous silicon boron imide gels from single-source precursors via a nonaqueous sol-gel route," *Chem. Mater.*, **15** [24], 4651-4657 (2003); C. Balan, K. W. Völger, E. Kroke and R. Riedel, "Viscoelastic properties of novel silicon carbodiimide gels," *Macromolecules*, **33** [9], 3404-3408 (2000).

- 17 R. Riedel, G. Mera, R. Hauser and A. Klonczynski, "Silicon-based polymer-derived ceramics: Synthesis properties and applications - A review," *J. Ceram. Soc. Jpn.*, **114** [1330], 425-444 (2006); A. Hannemann, J. C. Schön and M. Jansen, "Modeling the sol-gel synthesis route of amorphous $\text{Si}_3\text{B}_3\text{N}_7$," *J. Mater. Chem.*, **15** [11], 1167-1178 (2005).
- 18 F. Cheng, S. M. Kelly, S. Clark, J. S. Bradley, M. Baumbach and A. Schütze, "Preparation and characterization of a supported Si_3N_4 membrane *via* a non-aqueous sol-gel process," *J. Memb. Sci.*, **280** [1-2], 530-535 (2006); K. W. Völger, R. Hauser, E. Kroke, R. Riedel, Y. H. Ikuhara and Y. Iwamoto, "Synthesis and characterization of novel non-oxide sol-gel derived mesoporous amorphous Si-C-N membranes, *J. Ceram. Soc. Jpn.*, **114** [1330], 567-570 (2006).
- 19 A. W. Jackson and A. L. Hector, "A nonoxidic sol-gel route to titanium nitride and carbonitride films by primary amine condensation," *J. Mater. Chem.*, **17** [10], 1016-1022 (2007).
- 20 S. Hassan, A. L. Hector, J. R. Hyde, A. Kalaji and D. C. Smith, "A non-oxide sol-gel route to synthesise silicon imidonitride monolithic gels and high surface area aerogels," *Chem. Commun.*, [42], 5304-5306 (2008).
- 21 B. Gray, S. Hassan, A. L. Hector, A. Kalaji and B. Mazumder, "Template infiltration routes to ordered macroporous TiN and SiN_x films," *Chem. Mater.* **21** [18], 4210-4215 (2009).
- 22 J. Löffelholz, J. Engering and M. Jansen, "Sol-gel-process in the ammono-system - a novel access to silicon based nitrides," *Z. Anorg. Allg. Chem.*, **626** [4], 963-968 (2000).
- 23 F. Cheng, S. M. Kelly, F. Lefebvre, S. Clark, R. Supplit and J. S. Bradley, "Preparation of a mesoporous silicon aluminium nitride *via* a non-aqueous sol-gel route," *J. Mater. Chem.*, **15** [7], 772-777 (2005); S. Kaskel, G. Chaplais and K. Schlichte, "Synthesis, characterization,

- and catalytic properties of high-surface-area aluminum silicon nitride based materials,” *Chem. Mater.*, **17** [1], 181-185 (2005).
- 24 F. Cheng, S. M. Kelly, S. Clark, N. A. Young, S. J. Archibald and J. S. Bradley, “Ammonothermal synthesis of a mesoporous Si-Ti-N composite material from a single-source precursor,” *Chem. Mater.*, **17** [22], 5594-5602 (2005).
 - 25 D. V. Baxter, M. H. Chisholm, G. J. Gamma, V. F. DiStasi, A. L. Hector and I. P. Parkin, “Molecular routes to metal carbides, nitrides, and oxides .2. Studies of the ammonolysis of metal dialkylamides and hexamethyldisilylamides, *Chem. Mater.*, **8** [6], 1222-1228 (1996).
 - 26 F. Cheng, S. Clark, S. M. Kelly and J. S. Bradley, “Preparation of mesoporous silicon nitride via a nonaqueous sol-gel route,” *J. Am. Ceram. Soc.*, **87** [8], 1413-1417 (2004).
 - 27 U. Schubert and N. Hüsing, “Synthesis of Inorganic Materials,” Wiley-VCH, Weinheim, 2000.
 - 28 L. Rebohle, J. von Borany, W. Skorupa, I. E. Tyschenko, H. Fröb and K. Leo, “Strong blue and violet photoluminescence and electroluminescence from germanium-implanted and silicon-implanted silicon-dioxide layers,” *Appl. Phys. Lett.*, **71** [19], 2809-2811 (1997).
 - 29 D. C. Bradley, J. S. Ghotra and F. A. Hart, “Low coordination numbers in lanthanide and actinide compounds. 1. Preparation and characterization of *tris[bis(trimethylsilyl)-amido]lanthanides*,” *J. Chem. Soc., Dalton Trans.*, [10] 1021-1027 (1973).
 - 30 S. Hayashi, K. Hayamizu, “Chemical-shift standards in high-resolution solid-state NMR (1) C-13, Si-29 and H-1 nuclei,” *Bull. Chem. Soc. Jpn.*, **64** [2], 685-687 (1991).
 - 31 G. Metz, X. Wu and S. O. Smith, “Ramped-amplitude cross-polarization in magic-angle-spinning NMR,” *J. Magn. Reson. A*, **110** [2], 219-227 (1994).

Table 1 PL peak positions and linewidths compared with related Tb³⁺ phosphors

Environment of Tb ³⁺ ion	⁵ D ₄ → ⁷ F ₆ / nm	⁵ D ₄ → ⁷ F ₅ / nm	FWHM of ⁵ D ₄ → ⁷ F ₅ / nm	⁵ D ₄ → ⁷ F ₄ / nm	⁵ D ₄ → ⁷ F ₃ / nm
SiN _x powder (this work)	491	545	11	591	625
SiN _x film ^{5,6}	491-494	547	12-20	590-593	623-625
SiO ₂ film ^{4,5}	487-491	541-547	15-16	588-590	620-623
c- BN powder ⁷	486	543	12	588	623
AlN film ^{8,11,12}	490-492	541-554	9-12	587-589	625-627
AlN powder ¹⁰	484	542	15	585	621
GaN film ¹²	487	541	6	583	623
GaN powder ¹³	480	550	9	580	620

Fig. 1 IR spectra of a typical Tb:SiN_x xerogel as obtained (top) and after pyrolysis at 800 °C (bottom). Peaks due to the HNEt₂.HCl by-product in the top spectrum are marked with asterisks.

Fig. 2 Cross-polarized ²⁹Si MAS-NMR spectrum of silicon nitride produced by pyrolysis of a SiCl(NEt₂)₃/NH₃ xerogel.

Fig. 3 SEM image of Tb:SiN_x containing 3.55 at% Tb. The SEM shows the mixture of spherical and powdery particles.

Fig. 4 TEM of Tb:SiN_x containing 3.55 at% Tb, showing the even density and lack of nanoparticles.

Fig. 5 Photoluminescence excitation (left, using 545 nm emission) and emission (right, 242 nm excitation) spectra for Tb:SiN_x containing 3.55 at% Tb. The sample was diluted with powdered NaCl for this measurement. Inset shows the same sample irradiated with a 240 nm UV lamp.

Fig. 6 Variation in the intensity of the ⁵D₄→⁷F₆ line with Tb concentration in the Tb:SiN_x phosphors.